Optical design, analysis and performances of the infrared and visible channels of the Warm Calibration Unit in METIS/ELT

T. Sharma, M. Rutowska, M. Wiest, S. Graf, L. Labadie,

et al.

Optical design, analysis, and performances of the infrared and visible channels of the warm calibration unit in METIS/ELT

T. Sharma, M. Rutowska, M. Wiest, S. Graf, L. Labadie, et al.

SPIE.

Optical design, analysis and performances of the infrared and visible channels of the Warm Calibration Unit in METIS/ELT

T. Sharma[a], M. Rutowska[a], M. Wiest[a], S. Graf[a], L. Labadie[a], Ch. Straubmeier[a], A. Eckart[a], S. Todd[b], T. Agocs[c], R. Stuik[c], B. Brandl[c], and F. Bettonvil[c]

[a]I. Physikalisches Institut, Universität zu Köln, Zülpicher Straße 77, 50937, Köln, Germany
[b]UK Astronomy Technology Centre, STFC, Royal Observatory, Edinburgh, EH9 3HJ, UK
[c]NOVA Optical Infrared Instrumentation Group at ASTRON, P.O. Box 2, 7990 AA Dwingeloo, The Netherlands

ABSTRACT

METIS, the mid-infrared imager and spectrograph for the wavelength range 2.9 -13.5 μm (astronomical L-, M- N- band), will be one of the three science instruments at the Extremely Large Telescope (ELT). It will provide diffraction-limited imaging, coronagraphy, high-resolution integral field spectroscopy, and low and medium-resolution slit spectroscopy. Within the international METIS consortium, the University of Cologne is responsible for the design, manufacturing, integration, and qualification of the Warm Calibration Unit (WCU) of the instrument. In this contribution, we present the current status of the optical design and principle of optical operation of the WCU. The main train of the WCU optics is based on a modified F/17.75 Offner relay, with the optical output parameters matching the plate scale, F-number, as well as the exit-pupil position and size of that of the ELT. We discuss the optical design, and tolerance analysis of the WCU relay optics as part of the Optics FDR review by ESO. In addition, we present the concept and design of the Invar mechanical mounts for the WCU Zerodur mirrors, which are expected to undergo thermal and mechanical stresses. Finally, we present the optical design and analysis of the visible channel of the WCU that is aimed at alignment verification, as well as visualization of the METIS focal and pupil planes.

Keywords: METIS, Mid-Infrared, WCU, Calibration, Optical design, Tolerance Analysis.

1. INTRODUCTION

METIS[1,2](https://elt.eso.org/instrument/METIS/) will be one of three science instruments along with HARMONI and MICADO at the Extremely Large Telescope facility, presently under construction. The instrument is being built by a large consortium of European research institutions led by NOVA in the Netherlands with each partner responsible for a sub-system of the instrument. The individual subsystems will be tested at the responsible partner institute. The full assembly, integration, and testing of the instrument will take place in Leiden, before being shipped to the telescope site. In this process, the Warm Calibration Unit (WCU) is under development at the University of Cologne.[3,4] The primary role of the WCU is to provide artificial light sources mimicking the light coming from the telescope, which can be used to calibrate the instrument. In this paper, we describe the optical design aspects of the WCU along with the tolerance analysis and the lab experiments for WFE measurement. Lab experiments related to the Blackbody, aperture wheel are described by Graf et.al.[5] METIS is presently scheduled to undergo the Final Design Review (FDR) towards the end of 2022.

Sec. 2 provides the general view of the WCU. Optical design of the instrument and the tolerance analysis is described in Sec. 3. The same Sec. 3 also explains the mirror mount design and the effect of mirror clamping on the SFE. We detail the alignment optics part of the instrument in Sec. 4, tolerance analysis and results are also presented in the same section. Sec. 5 describes the results of the WFE measurement for test setup. Finally, we make the concluding remarks in Sec. 6.

Further author information: (Send correspondence to Tarun Kumar Sharma)
Tarun Kumar Sharma.: E-mail: sharma@ph1.uni-koeln.de, Telephone: +49 221 470 7791
Lucas Labadie.: E-mail: labadie@ph1.uni-koeln.de, Telephone: +49 221 470 3493

2. WARM CALIBRATION UNIT

The Warm Calibration Unit is a METIS subsystem, whose main role is to provide the METIS with a stable and controllable reference signal that will allow to troubleshoot and calibrate the response of the METIS in all the offered observing modes. This calls for a mechanical and an optical interface between the WCU and the METIS under the constraints of the ELT design. Additionally, the WCU must deliver the functionalities required for monitoring, troubleshooting, and calibration. Fig. 1(a) shows the WCU as a part of the whole METIS instrument, which itself is located on the ELT Nasmyth platform. The main unit of the METIS instrument is a cryostat which is placed on a Warm Support Structure (WSS, fixed legs at the bottom of the instrument). The WCU is mounted at the top of the instrument with the help of six adjustable links forming a hexapod. This hexapod allows the WCU to be aligned itself to the METIS instrument within the required range. Cabinets (Grey boxes) located under the instrument houses the control electronics, which are part of the Instrument Control System (ICS).

Fig. 1(b) shows the internal structure of the WCU without the enclosure. The different parts of the instrument are marked with alphabets. All the components of the WCU are placed on CFRP bench (d), which itself is supported by six adjustable links forming a hexapod (k) The Blackbody source is indicated with (m), which feeds the Integrating sphere (c), with an aperture mask (b) placed in between. Other laser sources are fed to the WCU with fiber connection (a). WCU optics consists of 7 mirrors, which form the beam as per the requirements. The first mirror of the chain is placed on a linear stage (l), which allows switching between the calibration and alignment mode of operation. There is an accessible pupil plane (e) located between CM1 and CM2, which allows putting a pupil mask wheel. Alignment optics of the WCU is placed on a linear stage (i), which allows switching between pupil plane and focal plane alignment modes. The CCD camera for alignment optics is placed on a linear stage (h), which allows for focusing. The WCU feeds the METIS with an optical beam using a periscope arm, which can move up and down and is represented with (g) and (h).

(a) METIS Overview.

(b) WCU Overview.
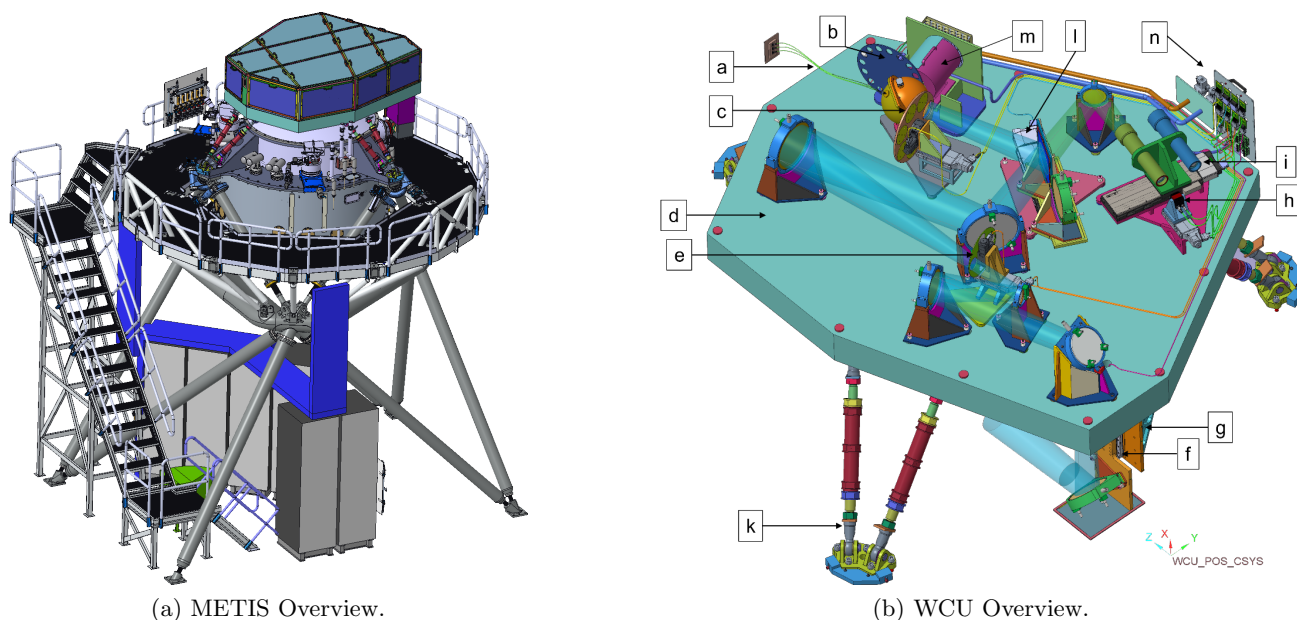
Figure 1: (a) Schematic overview of the current METIS design. WCU is at the top, mounted on the Cryostat, which is supported by the Warm Support Structure. Electrical cabinets are located at the bottom of the structure. (b) Overview of the main components of the WCU, semi-transparent blue cylinders represent the optical beam. WCU enclosure is not shown for better visualization of the internal components. Please note the 90° rotation between the two views. Important components on the bench are marked with alphabets.

3. WCU RELAY OPTICS

Fig. 2 shows the isometric view of the WCU relay optics, which is based on seven mirrors. Three of these mirrors are spherical while the remaining four are flat fold mirrors. Flat mirrors are used for folding the optical beam on the bench and bringing the beam to the instrument (METIS), while spherical mirrors are the ones that decides the optical properties of the beam, like the F-number.

The first two mirrors in the optical chain are Table Fold 1, and Table Fold 2 mirrors, which fold the light beam coming from the source (Integrating sphere and pinhole mask), towards the first spherical mirror (concave) CM1. The next mirror in the chain is the CM2 (convex). Between CM1 and CM2 is the accessible pupil plane, pupil plane masks are located here. Light reflected by the CM2 travels towards the next spherical mirror (concave) CM3, which reflects the light towards the periscope arm. The periscope arm has two flat mirrors, Fold down mirror and the Periscope feed mirror. All the mirrors are placed in the plane of the bench, except the periscope mirrors, which are at an angle of 45° from the bench plane. All seven mirrors are planned to be made of Zerodur glass, class 2, and coated with a protected gold coating. This glass is recommended for infra-red region and has a low CTE value as: $0 \pm 0.1 \times 10^{-6}$ mm/(mm·K). The clear aperture of the mirrors covers 10 % of the margin of FoV. For each mirror diameter, we have added an extra margin of 5 mm 10 mm, to allow for the mechanical mounting. Different color beams in Fig. 2 represents different fields, and Tab. 1 lists the optical fields and their coordinates for the nominal WCU optical design.
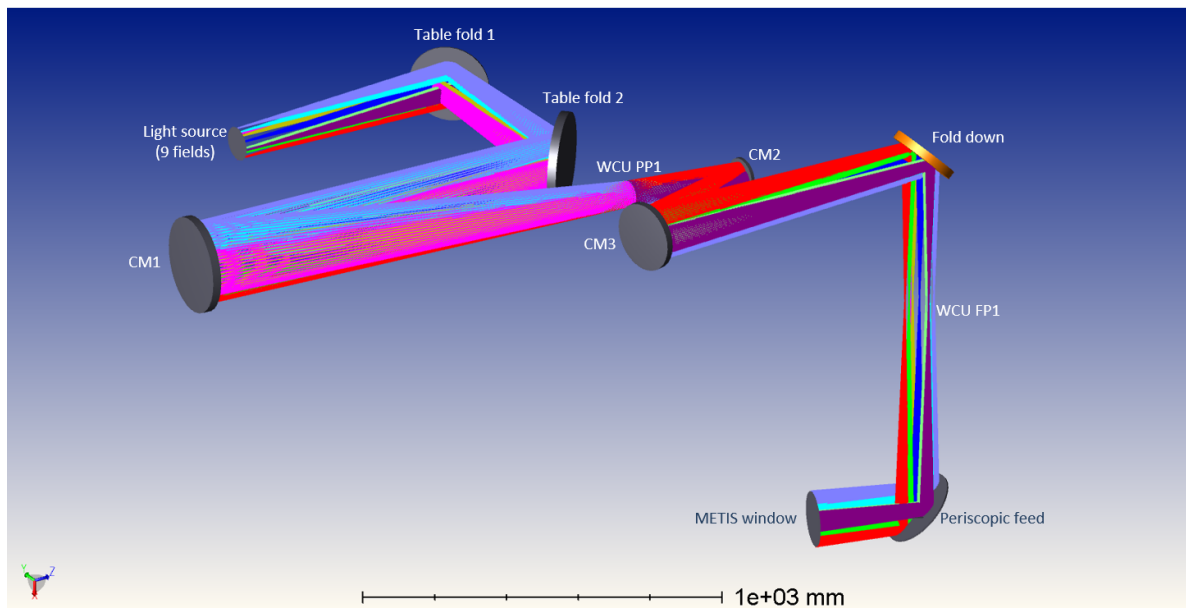

Figure 2: Isometric layout view of the WCU relay optics.

3.1 WCU Mirror Mounts and Effect of Mirror Clampling

Fig. 3 represents the design of the mirror mount for the CM1 mirror (mounted on the CFRP bench section), which is one of the largest mirror and has a spherical surface. The right side of the Fig. 3 shows the front side of the mirror (yellow) mount, which illustrates the protected gold coating. The clear aperture of the mirror is marked with a black circle of 248 mm in diameter. The center of the mirror is 287.5 mm in height from the bench top surface. The whole mirror mount is built around a triangular-shaped base plate. This base plate is mounted on the CFRP bench using a 3-point interface. These interfaces also compensate for any effect of differential CTE between the bench and the mount material. The mirror mount itself is held in its position using spring-loaded screws. Mirror mount up to the level of the mirror cell (the blue circular part surrounding the mirror) is made of the plate structure. There is a provision for shimming (small yellow parts between the blue mirror cell and the brown vertical plate) of the mirror cell to correct for the tilt, decenter, height, and axial shimming of the

Table 1: Optical fields and their coordinates for the nominal WCU optical design.

Field	Axis	Coordinate (mm)
Field 1	Origin	(0,0)
Field 2	+X	(34.142, 0)
Field 3	+X	(48.285, 0)
Field 4	+Y	(0, 34.142)
Field 5	+Y	(0, 48.285)
Field 6	-X	(-34.142, 0)
Field 7	-X	(-48.285, 0)
Field 8	-Y	(0, -34.142)
Field 9	-Y	(0, -48.285)

mirror. The mirror is placed inside the mirror cell using cylindrical contacts between the mirror and the mirror cell. The mirror is held in its position radially using a spring-loaded plunger located at the top of the mirror cell. The axial location of the mirror is maintained using three spring-loaded plungers. The spring force for these plungers are decided based on factors like earthquake requirements, contact stress on the mirror, and the mirror deformation due to clamping. The planned material for the mounts is Invar36, which has the advantage of low CTE. A similar mounting concept is also utilized for other mirror mounts of the WCU relay optics.
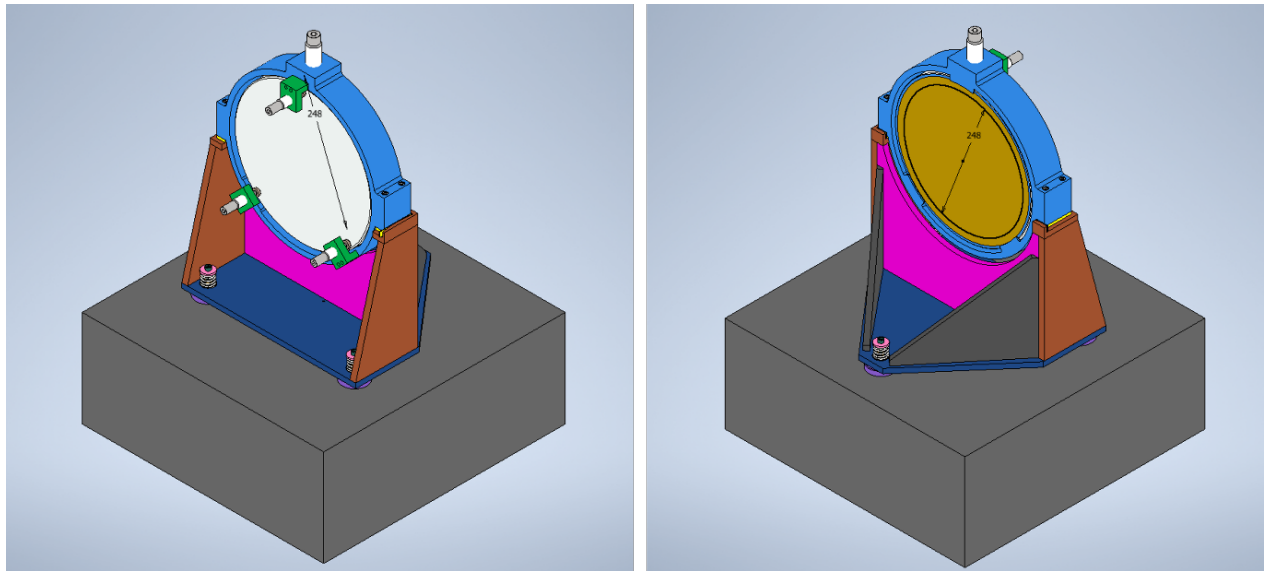

Figure 3: Representation of the CM1 mirror mount placed on a small section of the bench, at left side is the back view of the mirror mount and at right side is the front view of the mirror mount.

In the analysis presented in the next subsection, in all the cases of Gravity and temperature, only geometric parameters like mirror RoC, tilts, distances, etc. are accounted for. Mirror deformation due to mounting the mirror inside the mirror cell (with spring plungers) is not considered. To account for this effect in our WFE analysis, FEA models for all the mirrors mounted inside their mirror cells along with the proper axial and radial loads applied were prepared. This model was used to generate the deformed mirror surfaces, which were later used to calculate the WFE of the whole relay optics. Fig. 4 shows the example of one such case, where only Z-direction displacement of the mirror surface is shown for the CM1 mirror. Fig. 5 shows the resulting deformed
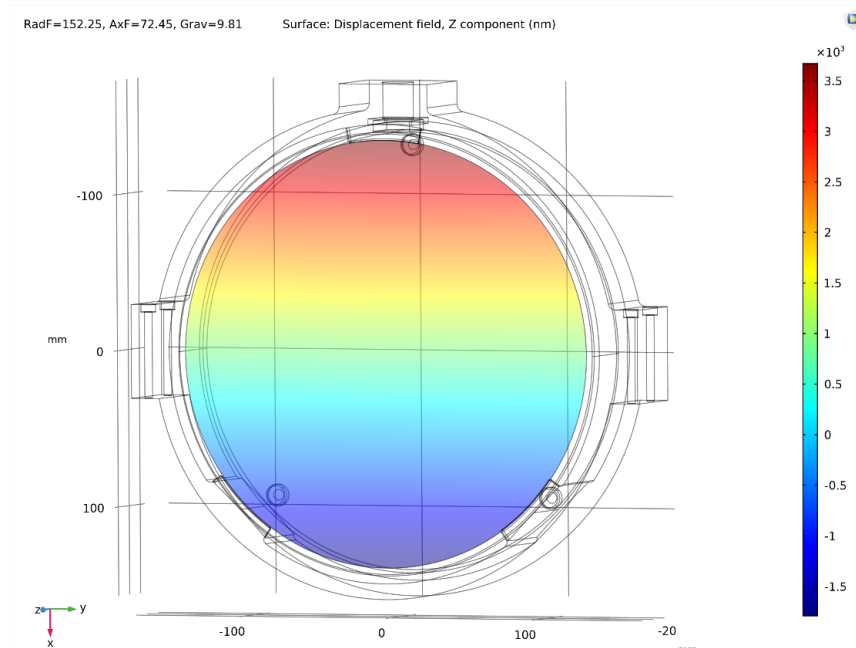
wavefront map for the CM1.

Figure 4: Z-displacement of the CM1 surface under axial and radial clamping loads.

A similar analysis was carried out for all the mirrors, and the resultant WFE was calculated when all the seven mirrors of the WCU relay optics are considered. Tab. 2 shows the result of this study in terms of Nominal WFE, Deformed WFE, and the Delta WFE for nine different fields.

Table 2: Nominal, Deformed and Delta WFE for the 9 fields, when considering clamping induced SFE for all the mirrors of the WCU relay optics.

Field	Nominal WFE (nm)	Deformed WFE (nm)	Delta WFE (nm)
Field 1	11.1	13.6	6.9
Field 2	31.0	33.3	12.16
Field 3	42.5	15.2	15.9
Field 4	9.0	11.5	7.15
Field 5	6.4	10.3	8.07
Field 6	31.0	34.1	14.2
Field 7	42.5	46.1	17.86
Field 8	3.9	10.8	10.07
Field 9	17.0	16.2	-5.15

3.2 WCU Relay Optics Tolerance Analysis

An extensive tolerance analysis has been carried out for the WCU replay optics to understand the effects of manufacturing, optomechanical tolerances, static effects like gravity, and quasi-static effects like that of temperature on the optical quality of the system. All these studies are carried out using software tools like ZEMAX® Op-
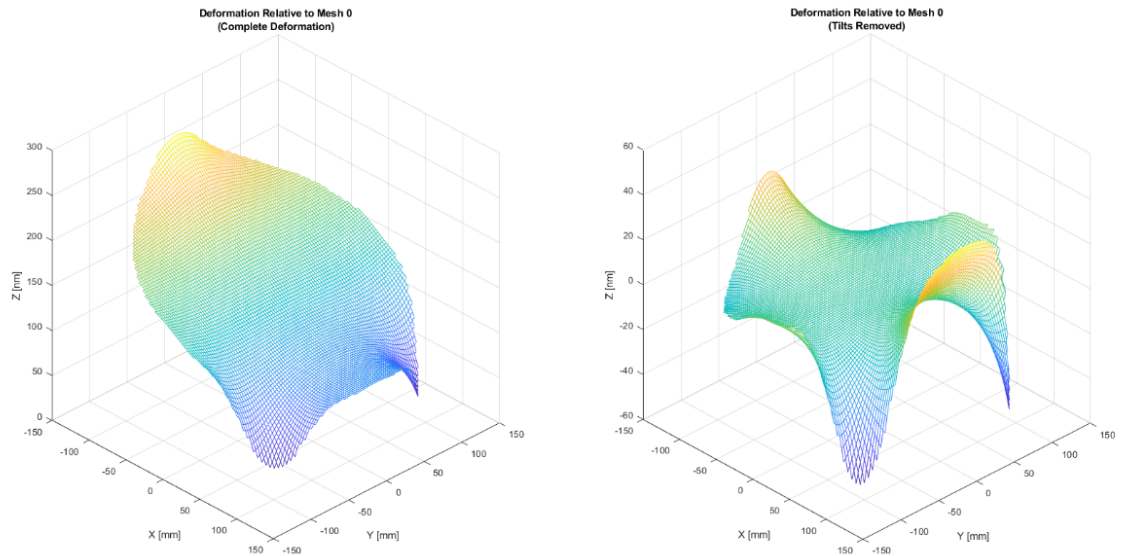
Figure 5: Deformed wavefront map for the CM1 under radial and axial clamping loads.

ticStudio, Inventor®, and COMSOL®. A number of analyses were carried out, which can be broadly classified under the following categories:-

1. Simulations where only static errors of the system are considered. These errors include manufacturing errors in mirrors such as tolerance on radius of curvature and errors related to the positioning of the optical components on the bench like tilts and shifts of the optical components. WFE due to SFE is calculated separately.

2. Simulation where deformation due to gravity is also considered along with the static errors mentioned in the previous point. Effect of gravity is simulated using the COMSOL® and Autodesk Inventor® (to cross check the results) and the resultant tilts, shifts and decenter terms are determined. These terms are added to the corresponding terms in the ZEMAX® model of the system, and then the performance is evaluated.

3. Simulations where deformation due to gravity and thermal effects is also considered along with the static errors. In this case, the combined effect of gravity and temperature is simulated in COMSOL®, and the resultant tilts, shifts and decenter terms are determined. These terms are added to the corresponding terms in the ZEMAX® model ofthe system, and then the performance is evaluated.

System parameters such as wavefront error, F-Number, shifts in focus, boresight error, exit pupil position, and diameter offsets are determined. However, only WFE is reported here, since it is the most important optical parameter. For all the simulations, the reference temperature for the WCU geometry is assumed as 20 °C. Fig. 6(a) shows the total displacement of the bench and the various components under the effect of gravity and temperature (i.e. when the ambient temperature is 10 degrees below the reference dimension temperature). The histogram plot of the RMS WFE for the same case is shown in Fig. 6(b).

As a next step, we calculate the total WFE when the effect of gravity, temperature, and mirror deformation due to clamping (Tab. 2) are all considered. WFE due to the clamping effect is added to the results using the Room Sum Squared (RSS) method. Tab. 3 lists the RMS WFE for the central field (Field 1) and four extreme fields. WFE for all the fields remains within 109 nm. However, for field 3, we see that the WFE is higher than
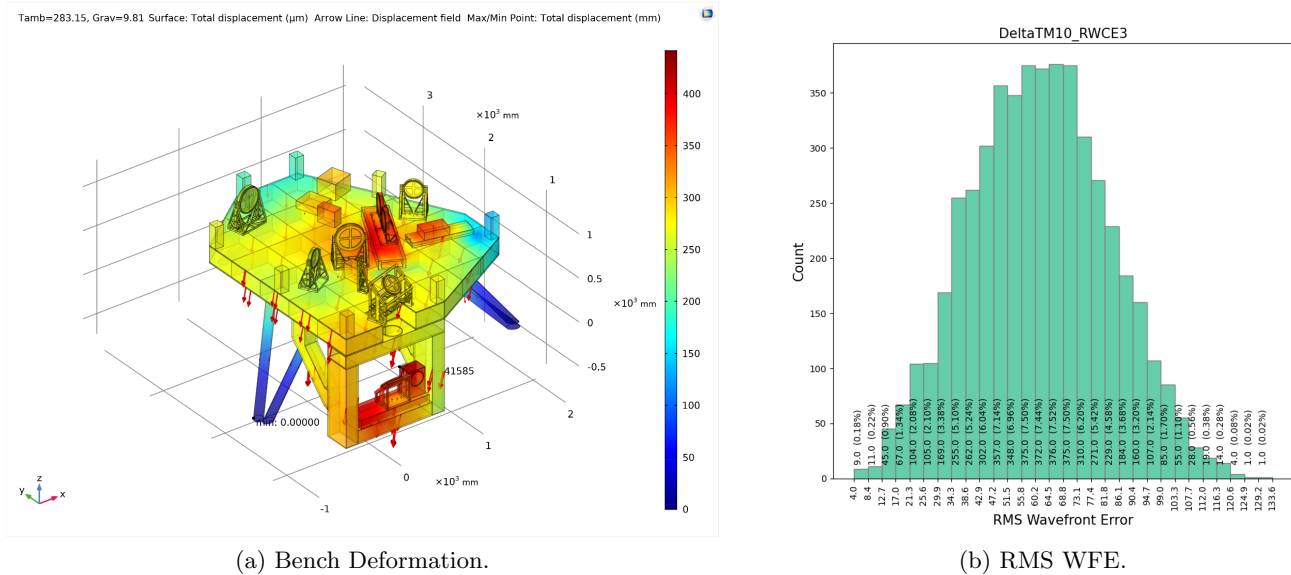
(a) Bench Deformation.

(b) RMS WFE.

Figure 6: (a) Total Displacement of the WCU bench and various components under the effect of Gravity and Temperature (Ambient Temperature 10 degrees below the reference dimension temperature). (b) Histogram plot for the RMS WFE for the simulation condition shown in left.

the requirement. The primary reason for this non-compliance for one field is the mechanical misalignment arising from gravity and temperature effects. Since the effect of gravity is static in nature, we plan to compensate for this by pre-shimming the mirror mounts (especially the spherical mirrors) in the vertical direction.

Table 3: Total wavefront error for the central field (**Field 1**) and four extreme fields under different conditions of gravity and temperature.

	Optical Tolerance WFE (nm)	**Only Gravity WFE (nm)**	**Gravity with $\triangle T = -10\ ^\circ C$ WFE (nm)**	**Gravity with $\triangle T = -20\ ^\circ C$ WFE (nm)**	**Gravity with $\triangle T = +10\ ^\circ C$ WFE (nm)**
Field 1	89.72	93.97	91.76	94.16	96.68
Field 3	109.5	118.96	119.31	125.27	119.31
Field 7	109	89.95	85.99	88.28	88.77
Field 5	82.52	101	99.44	94.39	104.77
Field 9	97.88	98.45	103.92	110.39	97.14

4. WCU ALIGNMENT OPTICS

For alignment checks during AIT and AIV phases, the WCU provides a visible light CCD operating at the wavelength range of 600 nm - 700 nm, which can image either the internal focal planes or pupil planes of the WCU, the CFO, and the different cameras of the METIS. The visible light required for this mode of operation is generated by the Blackbody source, which is heated to 1000 °C. Fig. 7 shows the integrating sphere illuminated with visible light generated by the Blackbody source. The visible light camera is located at the object plane FP2.2 of the WCU (see Fig. 1) and uses a monochrome Allied Vision Prosilica GT4907 36×24 mm^2 CCD with 4864×3232 pixels of 7.4×7.4 μm^2 size. The CCD is mounted at a fixed position on the optical bench of the WCU (on a small-range remotely controlled precision linear stage, however, to allow for proper focussing) and

two sets of remotely controlled exchangeable fore-optics of equal length ounted on a linear stage, that allows to switch between the focal-plane imaging mode and the pupil plane imaging mode. Design and tolerance analysis work for the Focal plane and Pupil plane optics is carried out using ZEMAX® OpticStudio.
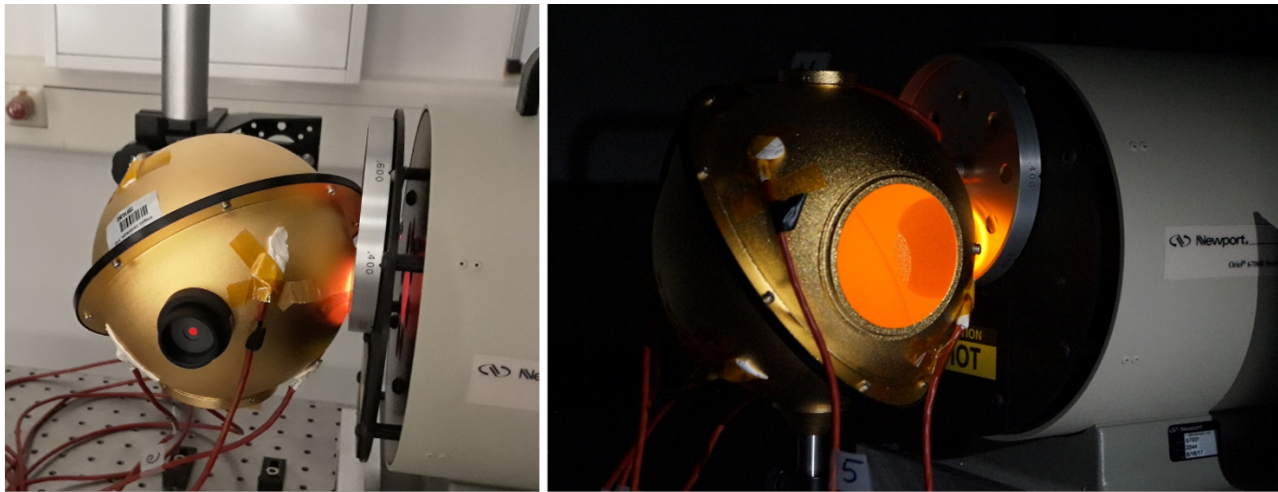

Figure 7: **Left:** Partly closed output of the integrating sphere. **Right:** Integrating sphere output port illuminated with visible light generated by the Blackbody source heated to 1000 °C.

4.1 WCU Focal Plane Viewing Fore-Optics

4.1.1 Requirements

The WCU shall allow focal plane within METIS to be imaged at visible wavelength with thefollowing performance:

1. Magnification: CCD area to cover a field of view corresponding to at least 15 arcsec on-sky

2. Resolution: FWHM < 10 mas (on sky equivalent)

4.1.2 How Design Fulfill Requirements

Requirements mentioned above are fulfilled by following: -

1. Present design shown in Fig. 8 covers a FoV of 16 arcsec with 1 arcsec as margin

2. 16 arcses FoV is imaged over 24×36 mm^2 area of the CCD with 7.4 μm pixel size. This corresponds to 4.95 mas per pixel. This means 2×2 pixel array is 9.9 mas (<10 mas). Nominal design puts all the rays in the 2×2 pixel size (also in the airy disk which is smaller than 2×2 pixels, see Fig. 9).

4.1.3 Focal Plane Viewing Fore-Optics: Nominal Design

Fig. 8 shows the ZEMAX® optical layout of the 5-lens fore-optics of the visible camera (WCU relay optics is not shown). All the lens materials are chosen from the SCHOTT® glass catalog. The fore-optics relays the 16 arcsec FoV of the WCU (96.57×96.57 mm^2) from its internal object plane FP2.2 onto the CCD of the camera (24×24 mm^2). As can be seen in the ZEMAX® spot diagrams in Fig. 9, the RMS spot size of the fore-optics is very close to the pixel size of the CCD of 7.4μm and the image quality is diffraction limited. The resolution of the images of the focal plane can thus be given by the number of pixels of the CCD across it. The vertical scale bar in Figure 4 is 14.8 μm, which is equal to the size of two pixels on the CCD camera. FoV of 16 arcsec is imaged on a sensor size of 24 mm×24 mm, this corresponds to 4.95 mas/pixel. This means, that 2 pixels cover 9.9 mas (<10 mas requirement). Also, note that the airy disk size is less than two pixels, and so is the spot size (diffraction-limited). Hence, the present design satisfies both the FoV and the resolution requirements in its nominal form.
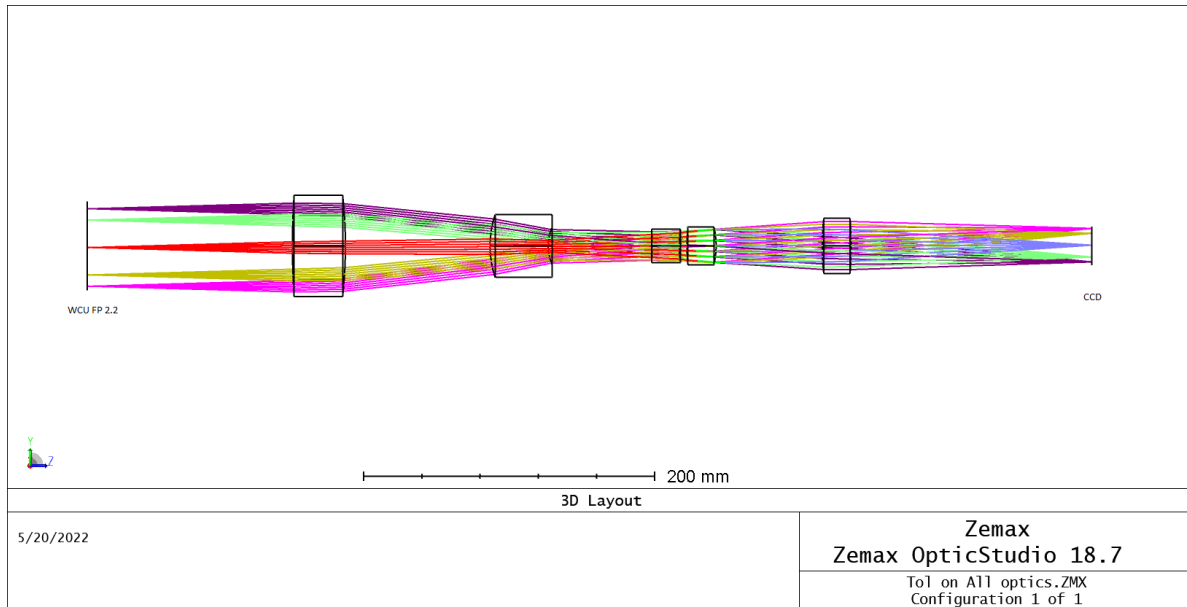
Figure 8: Zoomed view of the Focal Plane Viewing Fore-Optics.

4.1.4 Optical Tolerance Analysis

Optical tolerance analysis is run in ZEMAX® OpticStudio. Our analysis includes tolerances on all the elements of the Focal Plane Viewing Fore-Optics (all five lenses) and all the elements of the WCU relay optics except the periscope fold mirror. Additionally, Table Fold 1 mirror is not considered in this analysis as this is replaced with a beam splitter when WCU is operating in the alignment mode. Tilt/Decenter of surfaces, the distance between surfaces, tolerance on the radius of curvature for curved surfaces, and surface form error (using TEZI parameters) are some of the parameters which are used for this tolerance analysis. Tab. 4 lists the simulation setup parameters and the parameters used for the tolerance analysis. Since the total number of variables (parameters in the tolerance data editor) is 120, 15000 Monte-Carlo cycles are run to achieve convergence. The location of the focal plane is used as a compensator for the tolerance analysis, to achieve the best possible RMS spot size (criteria are defined in the merit function editor).
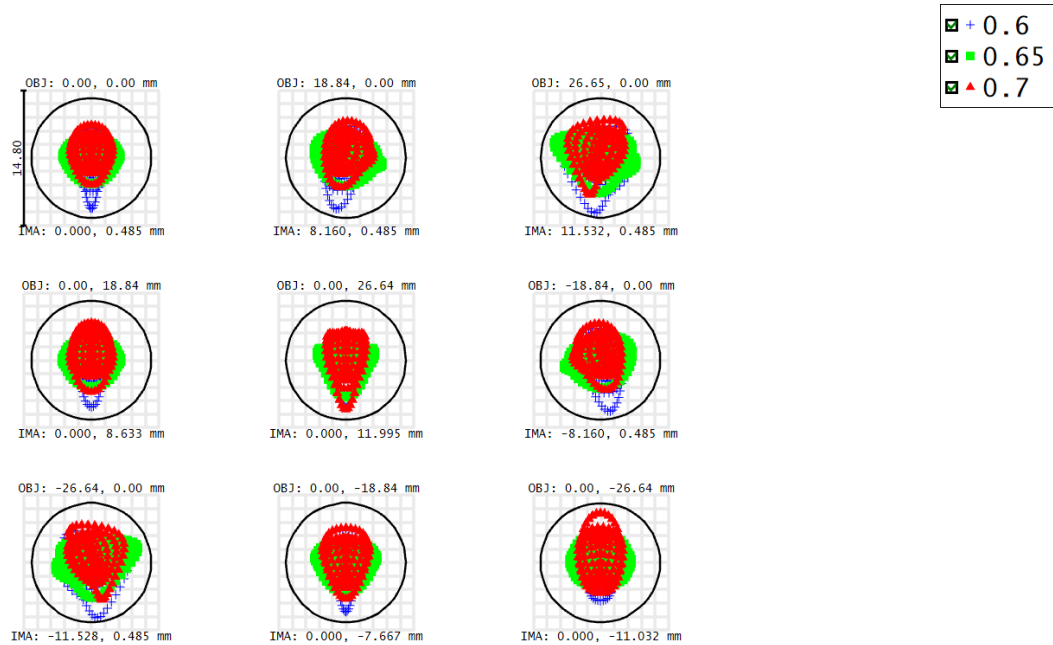
The simulation was set up to save the best and the worst cycles of the Monte-Carlo analysis. FFT PSF for the worst cycle of the analysis was plotted and FWHM values were determined. The FWHM values for all the 9 fields are listed in Tab. 5. Values listed in Tab. 5 are calculated for the sampling of 128×128, where each point is separated by 7.4 μm (pixel size of camera). It can be concluded from the Tab. 5 that the design meets the resolution requirement even when all the tolerances are considered. However, FWHM-Y for field 1 and field 4 is slightly larger than the requirement (requirement: 14.95 μm).

4.2 WCU Pupial Plane Viewing Fore-Optics

4.2.1 Requirements

The WCU shall allow pupils to be imaged at visible wavelengths with the following performance:

1. Magnification: CCD area to cover at least 100.5% of pupil diameter

2. Resolution (FWHM of PSF):

■ < 0.1% of the nominal pupil diameter over the central 50% of the pupil diameter

■ < 0.5% of the nominal pupil diameter over the complete pupil area

Figure 9: Nominal spot diagram for the different fields for the Focal Plane Viewing Fore-Optics.

4.2.2 How Design Fulfill Requirements

Requirements mentioned above are fulfilled by following: -

1. Design covers 101% of pupil diameter

2. 101% of pupil is imaged over 24×24 mm2 area of the CCD (3232×3232) with 7.4 μm pixel. This means about 3 pixels (22.2 μm) corresponds to 0.1% resolution (3232 pixels in one direction).

3. This resolution (<0.1%) is met over the whole pupil diameter, except for field point 6.

4.2.3 Pupil Plane Viewing Fore-Optics: Nominal Design

The design process of the fore-optics of the visible camera of the WCU for pupil plane imaging is not as straightforward as in the case for focal plane imaging, because the Offner relay introduces significant astigmatism when pupil imaging mode is used. This aberration has to be counteracted mainly by two means: by reducing the beam diameter (i.e. putting a stop in the focal plane of the WCU) and by allowing the optics to be not rotationally symmetric (i.e. allowing the lenses to be de-centered and tilted with respect to the optical axis).

The field of view requirement for WCU pupil plane imaging is that at least 100.5% of the pupil diameter shall be imaged. The resolution requirement for WCU pupil plane imaging is that theresolution is 0.1% of the full diameter of the pupil for first 50% and 0.5% for the remaining pupil. Since the CCD has more than 3200 pixels (exact 3223 pixels), this resolution requirement is fulfilled even if the observed PSF of a point source in

Table 4: Parameters used for the Focal Plane and the Pupil Plane Viewing Fore-Optics tolerance analysis.

Parameter	Value (Focal Plane)	Value (Pupil Plane)
Number of Monte Carlo cycles	15000	15000
Type of statistics	Normal	Normal
Total number of variables	120	120
Difference calculation method	Linear	Linear
Polynomial	No Polynomial	No Polynomial
Tolerance on RoC (all elements)	$\pm 0.1\%$	$\pm 0.1\%$
Thickness tolerance (μm, distance between two consecutive surfaces) (for Focal Plane Viewing Fore-Optics elements)	± 100	± 100
Thickness tolerance (μm, distance between two consecutive surfaces) (for relay optics elements)	± 140	± 140
Decenter tolerance (μm, for all the elements)	± 100	± 100
Tilt Tolerance (Beam splitter)	$\pm 0.014°$	$\pm 0.014°$
Tilt Tolerance (lens elements)	$\pm 0.025°$	$\pm 0.025°$
Tilt Tolerance (WCU relay optics elements)	$\pm 0.023°$	$\pm 0.023°$
Surface form error (using TEZI parameter, for all the elements)	± 15nm RMS	± 15nm RMS
Type of compensator	Location of the focal plane from the last element (CCD location)	Location of the focal plane from the last element (CCD location)

the pupil is spread over three pixels when the full pupil is imaged on the detector. Reducing the diameter of the beam in the focal plane to 68 mm (i.e. putting a respective stop in the focal plane) reduces the introduced aberrations of the Offner relay to a manageable level, but increases the diameter of the Airy disk to 2 pixels. However, this diameter is still within the requirement. The remaining aberrations are counteracted by allowing the lenses to be de-centered and tilted with respect to the optical axis. It should be noted that the individual lenses themselves still remain spherical and rotationally symmetric.

Fig. 10 shows the ZEMAX® optical layout of a 4-lens fore-optics for the WCU visible camera for pupil plane imaging following the two measures mentioned above. All the lens materials are from the SCHOTT® glass catalog. All 4 lenses are de-centered and tilted with respect to the nominal optical axis. The fore-optics relays the 101% of the full pupil diameter (the respective requirement is at least 101.5%) of the exit pupil of the ELT onto the CCD of the camera. As can be seen in theZEMAX® spot diagrams in Fig. 11, the Airy diameter of the fore-optics of 10 μm is smaller than the size of 2 detector pixels with 14.8 μm. Even over the full diameter of the pupil, the image quality is close to the diffraction limit for most of the fields, thus leaving even some margin to the given resolution requirement (the scale bar in Figure 6 represents the area of 3×3 detector pixels).

4.2.4 Optical Tolerance Analysis

Optical tolerance analysis is run in ZEMAX® OpticStudio. Our analysis includes tolerances on all the elements of the Pupil Plane Viewing Fore-Optics (all four lenses) and all the elements of the WCU relay optics except

Table 5: FWHM values of the FFT PSF for different fields of the worst-case cycle of the Monte-Carlo Tolerance Analysis for the Focal Plane Viewing Fore-Optics.

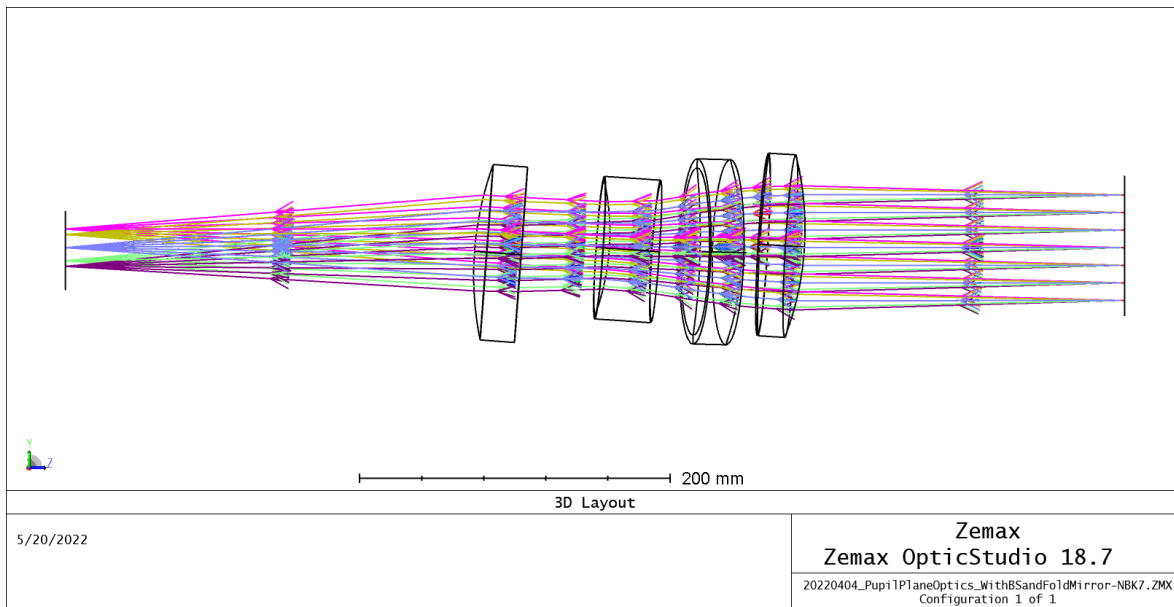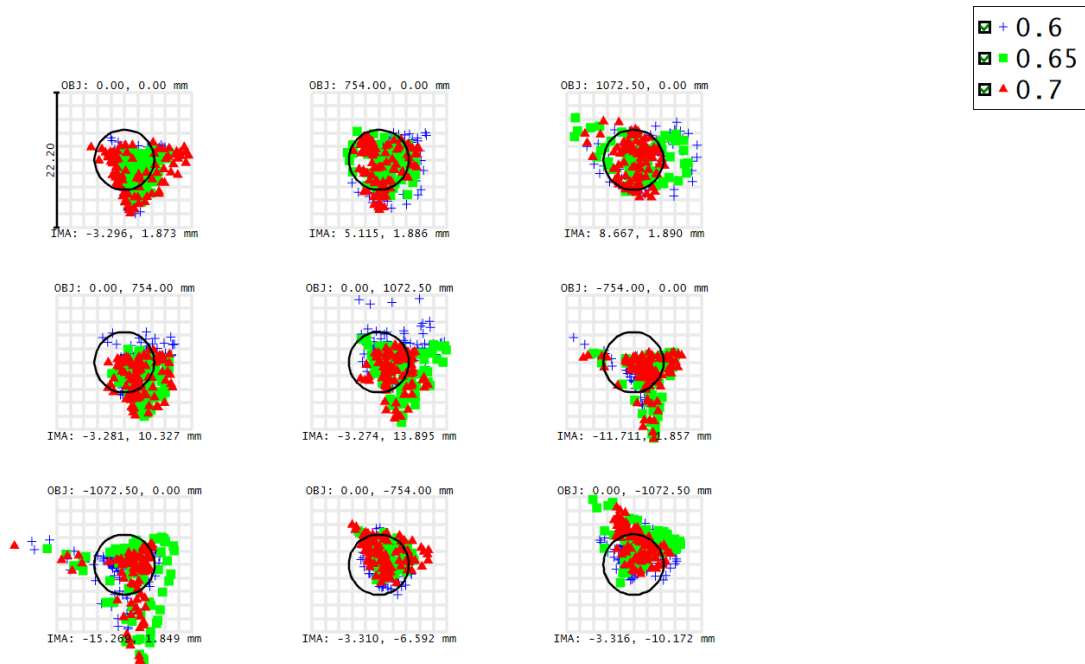| Field	FWHM-X (μm)	FWHM-Y (μm)
Field 1	6.58	15.30
Field 2	9.35	9.61
Field 3	9.78	9.30
Field 4	5.8	17.36
Field 5	5.37	12.20
Field 6	5.94	8.57
Field 7	7.34	14.26
Field 8	9.52	13.99
Field 9	8.59	13.70

Figure 10: Zoomed view of the Pupil Plane Viewing Fore-Optics.

the periscope fold mirrors. Additionally, Table Fold 1 mirror is not considered in this analysis as this is replaced with a beam splitter when WCU is operating in the alignment mode. Tilt/Decenter of surfaces, the distance between surfaces, tolerance on the radius of curvature for curved surfaces, and surface form error (using TEZI parameters) are some of the parameters which are used for this tolerance analysis. Tab. 4 lists the simulation setup parameters and the parameters used for the tolerance analysis. Since the total number of variables (parameters in the tolerance data editor) is 120, 15000 Monte-Carlo cycles are run to achieve convergence. The location of the focal plane is used asacompensator for the tolerance analysis, to achieve the best possible RMS spot size (criteria are defined in the merit function editor). The simulation was set up to save the best and the worst cycles of the Monte-Carlo cycles. FFT PSF for the worst cycle of the analysis was plotted and FWHM values were determined. The FWHM values for all the 9 fields are listed in Tab. 6. Values listed in Tab. 6 are calculated for the sampling of 128×128, where each point is separated by 7.4 μm (pixel size of camera). It can be concluded from Tab. 6 that the design meets the resolution requirement even when all the tolerances are considered. However, FWHM-Y for field 6 is slightly larger than 22.2 μm (although resolution requirements are

Figure 11: Nominal spot diagram for the different fields for the Pupil Plane Viewing Fore-Optics.

still met, 0.5% for the remaining 50% of the field).

5. LAB EXPERIMENTS

The most challenging requirement for the WCU in terms of optical quality is the RMS WFE, which is not supposed to exceed 109 nm (for 95% confidence level). This calls for the physical measurement of the WFE, once the whole WCU is assembled. At UzK, a Fisba Interferometer is available with us, which allows us to accurately measure the WFE. Since the whole WCU alignment strategy relies on the manufacturing tolerances and the measurement reports for individual parts, replication of such a strategy on a smaller scale along with WFE measurement seems a way forward.

For this, at UzK, we have prepared a setup consisting of a Fisba interferometer, two spherical mirrors (RoC of 1500 mm), and a flat mirror. Fisba interferometer outputs a 50 mm collimated beam as shown in Fig. 12(a), which falls on a spherical mirror. The second spherical mirror is conjugated with the first, so the beam reflected by the second spherical mirror is nearly collimated. The beam now travels to a flat mirror, which reflects the beam, making it follow its original path in the reverse direction. The light beam then enters the Fisba interferometer and produces the interference pattern.

An optical model of the setup shown in Fig. 12(a) was prepared in ZEMAX, and tolerance analysis was run. The tolerance parameters for this simulation were the tolerance on Roc of mirrors, tilts, decenter, distances between mirrors, and the surface form error for the mirrors. RMS wavefront error was observed for this analysis. Fig. 12(b) histogram plot for the RMS WFE for 5000 cycles of the Monte-Carlo analysis. RMS WFE for the

Table 6: FWHM values for the FFT PSF for the different fields of the worst-case cycle of the Monte-Carlo Tolerance Analysis for the Pupil Plane Viewing Fore-Optics.

Field	FWHM-X (μm)	FWHM-Y (μm)
Field 1	8.58	14.12
Field 2	5.27	1.38
Field 3	5.54	9.88
Field 4	7.13	9.95
Field 5	9.37	15.6
Field 6	17.18	24.17
Field 7	14.39	12.5
Field 8	5.48	11.31
Field 9	5.42	11.95
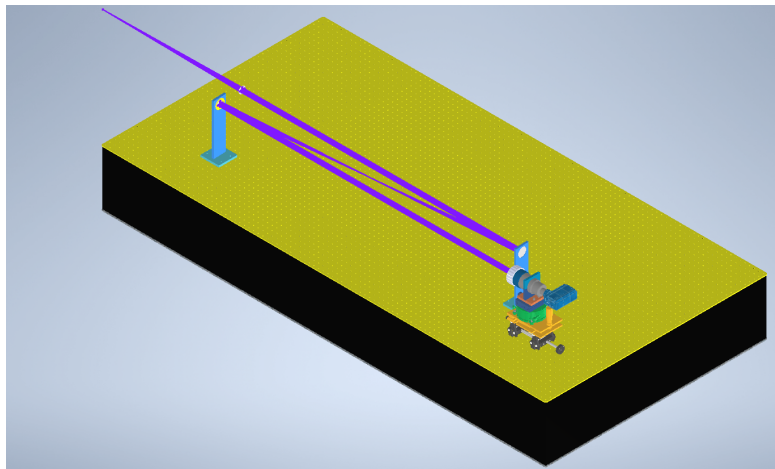
(a) Experimental setup.
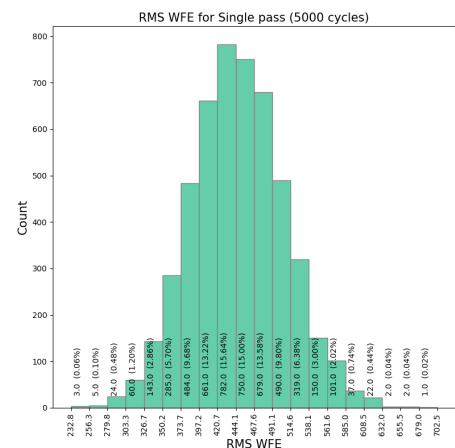
(b) RMS WFE(nm).

Figure 12: (a) CAD model of the lab setup consisting of Fisba interferometer, two conjugated spherical lenses (RoC of 1500 mm) (b) Histogram plot of the RMS WFE (nm) for the Fisba setup from the tolerance analysis involving manufacturing tolerances for the mirrors and the mounts.

95% confidence level is at 546.88 nm. It is important to note here that the simulation considers only a single pass of the beam, while in reality, the beam passes two times between the Fisba and the reference mirror (not shown in Fig. 12(a)). This calls for a multiplication factor of 2, and the new RMS WFE for 95% confidence level is 1093.76 nm.

Fig. 13 shows the screenshot image of the Fisba measurement window. One can see from the Fig. 13 that the major component of the WFE is the defocus, which is expected since the two lenses are not perfectly conjugated. The measured RMS WFE is about 698 nm, below the maximum allowable RMS WFE of 1093.76 nm. We would like to point out that the WFE due to the reference mirror is already removed from the measurement results by the initial calibration process, and including the calibration into the measurement.

6. CONCLUSION

The optical design of the WCU relay optics has been presented along with the associated tolerance analysis. The design of the mirror mount and the effect of the clamping forces on the RMS WFE has been analyzed and
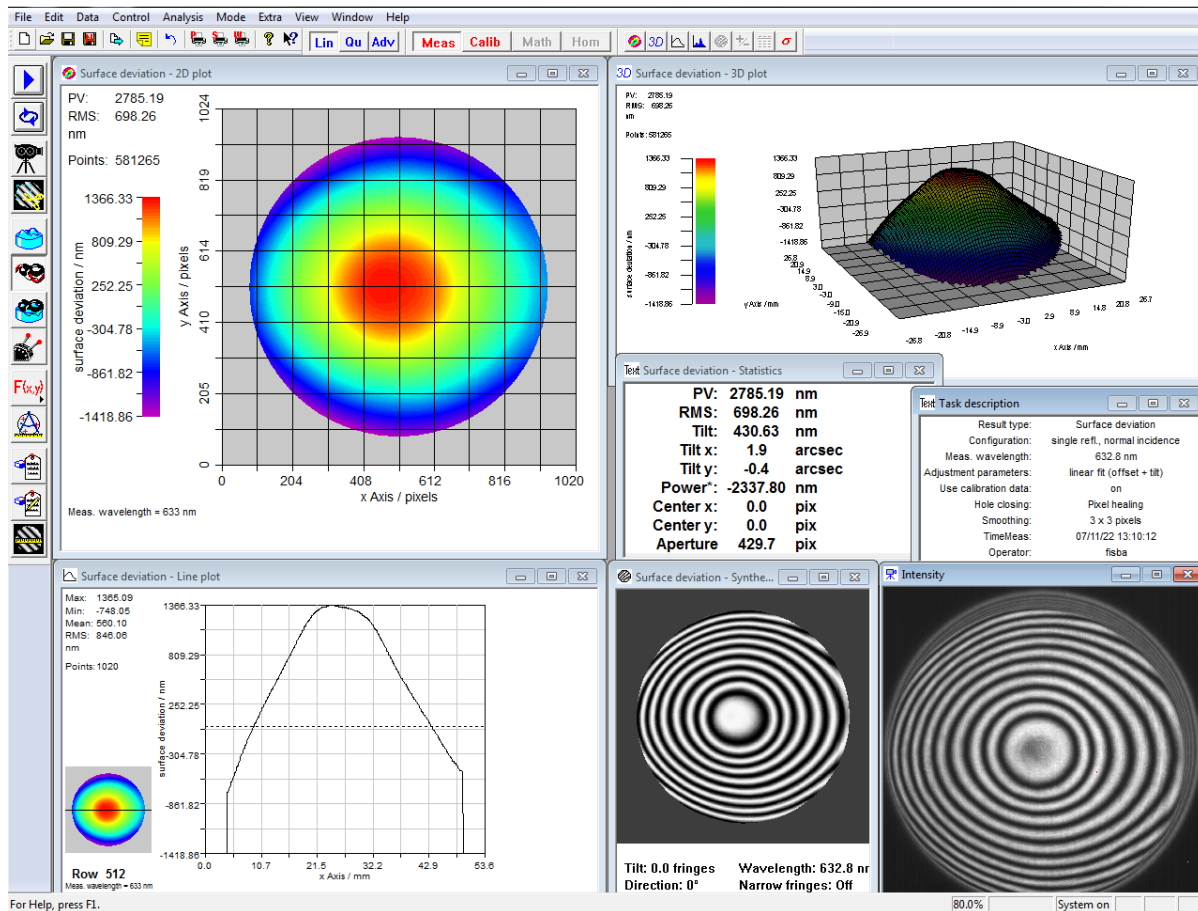
Figure 13: Screenshot image of the Fisba measurement window.

discussed. Optical design of the two channels of the alignment optics, i.e. the focal plane optics and the pupil plane optics is described and the effect of the tolerances on their performance has been discussed. Experimental results from a test setup for WFE measurement has been reported.

ACKNOWLEDGMENTS

REFERENCES

[1] Brandl, B. R., Absil, O., Agócs, T., Baccichet, N., Bertram, T., Bettonvil, F., van Boekel, R., Burtscher, L., van Dishoeck, E., Feldt, M., Garcia, P. J. V., Glasse, A., Glauser, A., Güdel, M., Haupt, C., Kenworthy, M. A., Labadie, L., Laun, W., Lesman, D., Pantin, E., Quanz, S. P., Snellen, I., Siebenmorgen, R., and van Winckel, H., "Status of the mid-IR ELT imager and spectrograph (METIS)," in [*Ground-based and Airborne Instrumentation for Astronomy VII*], Evans, C. J., Simard, L., and Takami, H., eds., *Society of Photo-Optical Instrumentation Engineers (SPIE) Conference Series* **10702**, 107021U (July 2018).

[2] Brandl, B., Bettonvil, F., van Boekel, R., Glauser, A., Quanz, S., Absil, O., Amorim, A., Feldt, M., Glasse, A., Güdel, M., Ho, P., Labadie, L., Meyer, M., Pantin, E., van Winckel, H., and METIS Consortium, "METIS: The Mid-infrared ELT Imager and Spectrograph," *The Messenger* **182**, 22–26 (Mar. 2021).

[3] Baccichet, N., Labadie, L., Rost, S., Straubmeier, C., Agócs, T., Jellema, W., Reolfsema, R., van Boekel, R., Glauser, A., Brandl, B., Bettonvil, F., Lynn, J., and Eckart, A., "The calibration unit of the mid-infrared E-ELT instrument METIS," in [*SPIE proceedings,Ground-based and Airborne Instrumentation for Astronomy VII*], Evans, C. J., Simard, L., and Takami, H., eds., **1070291**, 990820 (July 2018).

[4] Rutowska, M., Sharma, T., Wiest, M., Graf, S., Straubmeier, C., Rost, S., Labadie, L., Eckart, A., Burtscher, L., Agcs, T., Lesman, D., Stuik, R., Glauser, A., Brandl, B., and Bettonvil, F., "Warm calibration unit of the mid-infrared E-ELT instrument METIS: overview and current status of the project," in [*Ground-based and Airborne Instrumentation for Astronomy VIII*], Evans, C. J., Bryant, J. J., and Motohara, K., eds., **11447**, 586 – 596, International Society for Optics and Photonics, SPIE (2020).

[5] Graf, S., Rutowska, M., Wiest, M., Rost, S., Straubmeier, C., and Labadie, L., "The warm calibration unit of METIS: laboratory tests and proof-of-concept," in [*Society of Photo-Optical Instrumentation Engineers (SPIE) Conference Series*], *Society of Photo-Optical Instrumentation Engineers (SPIE) Conference Series* **11447**, 114472R (Dec. 2020).